Metabonomic Characterization of Genetic Variations in Toxicological and Metabolic Responses Using Probabilistic Neural Networks

ARTICLE *in* CHEMICAL RESEARCH IN TOXICOLOGY · FEBRUARY 2001

Impact Factor: 3.53 · DOI: 10.1021/tx000158x · Source: PubMed

3 AUTHORS, INCLUDING:

Elaine Holmes
Imperial College London
458 PUBLICATIONS **29,215** CITATIONS

SEE PROFILE

Jeremy K Nicholson
Imperial College London
740 PUBLICATIONS **43,846** CITATIONS

SEE PROFILE

Metabonomic Characterization of Genetic Variations in Toxicological and Metabolic Responses Using Probabilistic Neural Networks

Elaine Holmes, Jeremy K. Nicholson, and George Tranter*

Biological Chemistry, Biomedical Sciences Division, Imperial College of Science, Technology and Medicine, Exhibition Road, London SW7 2AZ, U.K.

Received July 25, 2000

Current emphasis on efficient screening of novel therapeutic agents in toxicological studies has resulted in the evaluation of novel analytical technologies, including genomic (transcriptomic) and proteomic approaches. We have shown that high-resolution ^{1}H NMR spectroscopy of biofluids and tissues coupled with appropriate chemometric analysis can also provide complementary data for use in in vivo toxicological screening of drugs. Metabonomics concerns the quantitative analysis of the dynamic multiparametric metabolic response of living systems to pathophysiological stimuli or genetic modification [Nicholson, J. K., Lindon, J. C., and Holmes, E. (1999) *Xenobiotica* **11**, 1181−1189]. In this study, we have used ^{1}H NMR spectroscopy to characterize the time-related changes in the urinary metabolite profiles of laboratory rats treated with 13 model toxins and drugs which predominantly target liver or kidney. These ^{1}H NMR spectra were data-reduced and subsequently analyzed using a *probabilistic* neural network (PNN) approach. The methods encompassed a database of 1310 samples, of which 583 comprised a training set for the neural network, with the remaining 727 (independent cases) employed as a test set for validation. Using these techniques, the 13 classes of toxicity, together with the variations associated with strain, were distinguishable to >90%. Analysis of the ^{1}H NMR spectral data by multilayer perceptron networks and principal components analysis gave a similar but less accurate classification than PNN analysis. This study has highlighted the value of probabilistic neural networks in developing accurate NMR-based metabonomic models for the prediction of xenobiotic-induced toxicity in experimental animals and indicates possible future uses in accelerated drug discovery programs. Furthermore, the sensitivity of this tool to strain differences may prove to be useful in investigating the genetic variation of metabolic responses and for assessing the validity of specific animal models.

Introduction

There is great interest in the development of novel analytical technologies for rapid screening of biological dysfunction in pharmaceutical and clinical applications. Technologies such as proteomics, genomics, and transcriptomics are becoming integral components of drug discovery (*1*−*4*). However, these methods do not provide insight into the integrated function of a complex biosystem over time. Methods that provide a coherent perspective of the complete metabolic response of organisms to physiological and pathophysiological stimuli provide a complement to these techniques (*1*). We have shown that ^{1}H NMR[1] spectroscopy of biofluids and tissues provides an effective metabolic profile representing many key biochemical pathways in an organism and their modification with metabolic dysfunction (*5*−*8*). This has given rise to the "metabonomic" approach to toxicological evaluation, which we have defined as "the study of the multivariate time-resolved metabolic changes in biofluids, cells and tissues to pathophysiological insult or genetic modification" (*1*).

High-resolution ^{1}H NMR spectroscopy of ex vivo biofluids such as urine, plasma, and cerebrospinal fluid (*5*−*8*) is especially suitable for generating metabonomic data as the technique is rapid and nondestructive and allows information about a variety of metabolic pathways to be accessed simultaneously while little or no sample preparation is required (*1*, *8*). Likewise, magic angle spinning (MAS) NMR spectroscopy can be employed to study intact tissues.

^{1}H NMR spectra of biofluids are information-rich, and thus, pattern recognition and chemometric methods can be employed to maximize information recovery (*1*, *9*). To date, various methods of multivariate analysis have been applied to the interpretation of NMR biofluid data, including principal components analysis (PCA), nonlinear mapping analysis, and neural networks (*9*−*12*). These analyses showed that classification of liver, kidney, and testicular toxicity could be achieved and that each type of tissue-specific toxicity could be characterized by a combination of metabolite changes.

* To whom correspondence should be addressed.

[1] Abbreviations: BEA, 2-bromoethanamine; FID, free induction decay; HCBD, hexachlorobuta-1,3-diene; HW, Han Wistar; ip, intraperitoneal; NNs, neural networks; NMR, nuclear magnetic resonance; PR, pattern recognition; po, per oral; PCA, principal components analysis; PNNs, probabilistic neural networks; PAN, puromycin aminonucleoside; RPN, renal papillary necrosis; SD, Sprague-Dawley; UN, uranyl nitrate.

10.1021/tx000158x CCC: $20.00
Published on Web 01/23/2001

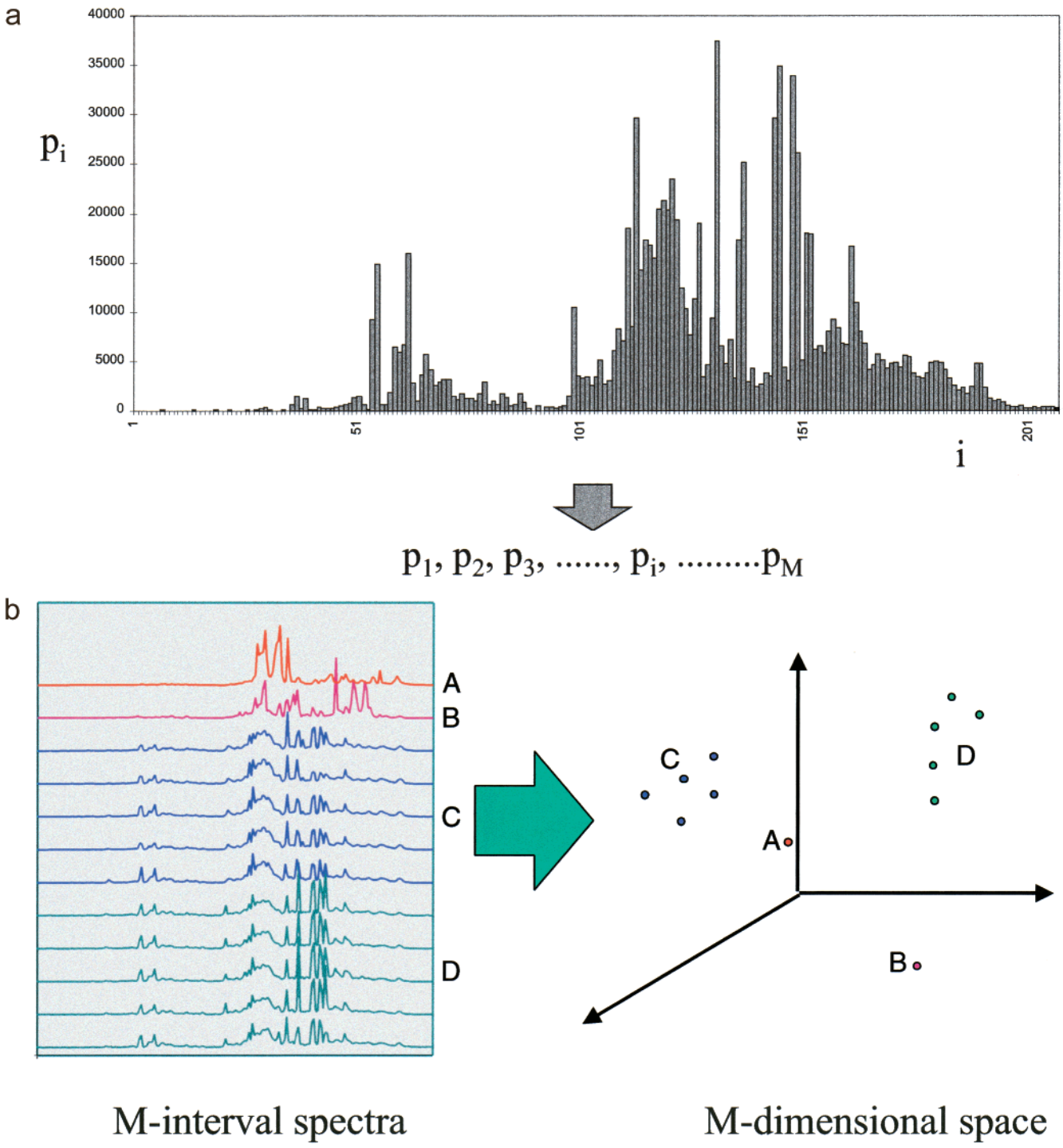

Figure 1. Spectra as vectors in a metabonomic space. (a) Schematic diagram of the digitization of a spectrum into input vector **p**. (b) Representation of spectra in *M*-dimensional space ($M = 3$ for illustration only).

The technique is a great improvement over histopathology, since having generated the metabonomic spectroscopic pattern recognition based on histopathological and clinical chemical results, future studies would only require collection of urine from experimental animals or humans. Thus, studies following the evolution in time of toxicological events can be pursued on individual rats without the need for killing animals at each time point. Consequently, variations in the behavior of individual animals can be better accounted for. Histopathology cannot carry detailed mechanistic information, but NMR gives biochemical information that can be related to metabolic dysfunction and hence to mechanisms. Many of the biomarkers detected by NMR in previous studies have been novel and have provided insight into mechanisms and processes of toxicity and disease (*1*, *5*, *12*).

Here we describe, for the first time, the use of probabilistic neural networks for achieving a much-improved classification of toxic responses, over more conventional multivariate analyses such as PCA and SIMCA (*13*), encompassing strain- and time-related variation from NMR spectra. Probabilistic neural networks (PNNs) provide a powerful method of analyzing data in terms of Bayesian probability distributions (*14*) and are particularly suited to highly nonlinear classification problems

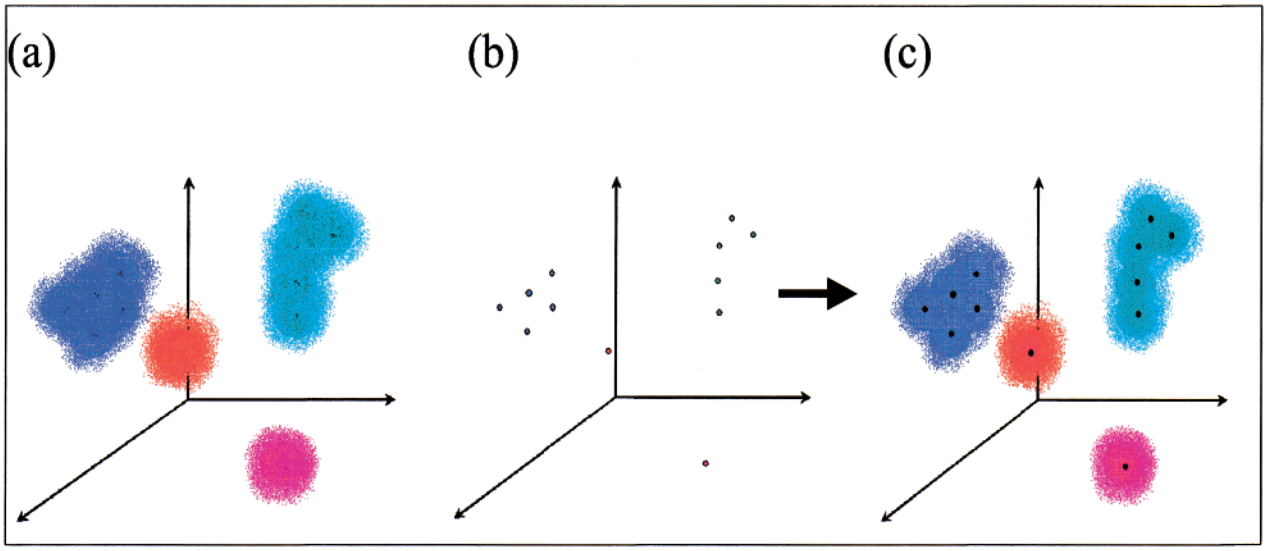

Figure 2. Construction of probability distributions for four classes in *M*-dimensional space: (a) actual distribution, (b) exemplar points from the training set, and (c) reconstruction of distribution using *M*-dimensional Gaussian distributions around exemplar points ($M = 3$ for illustration only).

Table 1. Indication of the Administered Compound, Dose Level, Strain of Rat, and Defined Region of Lesion Together with the Appropriate Training Categories for Initial and Refined Classification

administered compound	tissue that has been affected (as defined by histopathology)	strain and dose	class for initial study	class for refined study
control vehicle	none	HW (0.9% saline ip and po)	1	1
		SD (0.9% saline ip)	6	10
adriamycin	kidney cortex, liver, heart	SD (5 mg/kg ip)	8	14
α-naphthyl isothiocyanate (ANIT)	liver (cholestasis)	HW (90 mg/kg po)	2	3
		HW (100 mg/kg po)	2	3
allyl alcohol	liver (cholestasis)	HW (100 mg/kg po)	2	4
		HW (200 mg/kg po)	2	4
2-bromoethanamine (BEA)	mitochondria (<24 h)	HW (150 mg/kg ip)	5	8
		HW (250 mg/kg ip)	5	8
	kidney papilla (>24 h)	SD (250 mg/kg ip)	10	13
		HW (150 mg/kg ip)	4	9
		HW (250 mg/kg ip)	4	9
		SD (250 mg/kg ip)	9	16
dimethylhydrazine (DMH)	liver (centrolobular necrosis)	HW (30 mg/kg po)	2	6
		HW (100 mg/kg po)	2	6
hexachloro-1,3-butadiene (HCBD)	kidney cortex (S3)	HW (100 mg/kg ip)	4	7
		HW (200 mg/kg ip)	4	7
		SD (200 mg/kg ip)	9	11
hydrazine	liver (steatosis)	HW (90 mg/kg po)	2	2
		HW (120 mg/kg po)	2	2
lead acetate (PbAc)	liver, kidney	SD (98 mg/kg ip)	8	12
mercury(II) chloride ($HgCl_2$)	kidney cortex (S3)	HW (0.25 mg/kg ip)	4	7
		HW (0.75 mg/kg ip)	4	7
		SD (0.75 mg/kg ip)	9	11
puromycin aminonucleoside (PAN)	liver, kidney cortex (<72 h)	SD (150 mg/kg ip)	9	15
	kidney glomerulus (>72 h)	SD (150 mg/kg ip)	9	17
sodium fluoride (NaF)	kidney cortex (S1−3)	SD (35 mg/kg ip.)		18
		SD (45 mg/kg ip)	9	18
thioacetamide	liver, kidney	HW (100 mg/kg po)	3	5
		HW (100 mg/kg po)	3	5
uranyl nitrate (UN)	kidney cortex (S3)	SD (10 mg/kg ip)	9	11

(*15*−*17*). In particular, they make no assumption with respect to the detailed mathematical relationship between the input data (spectra) and the resulting classifications, this being dictated solely by the data itself. Unlike other neural networks (e.g., multilayer perceptrons), PNNs incorporate all of the information to be found in the data set while avoiding the problems of overfitting the data to achieve classification (*18*). In this study, NMR spectra of urine acquired from rats treated with a variety of tissue-specific toxins (based on histopathological evidence) were classified in terms of the site of action, mechanism of toxicity, and strain of rat.

Metabonomic Space and Probabilistic Neural Networks. A NMR spectrum digitized into *M* intervals along the frequency axis (as shown in Figure 1a) can be considered an *M*-dimensional vector. Thus, any spectrum can be represented as a unique point in *M*-dimensional space (Figure 1b). In this case, the vector is representative of the metabolic condition (the metabonomic profile) of the organism from which the sample derived at that particular time. If the spectra contain information about the class of toxicity (site or mechanism of action, rat strain, etc.), then throughout this space there will be corresponding probability distributions, one for each

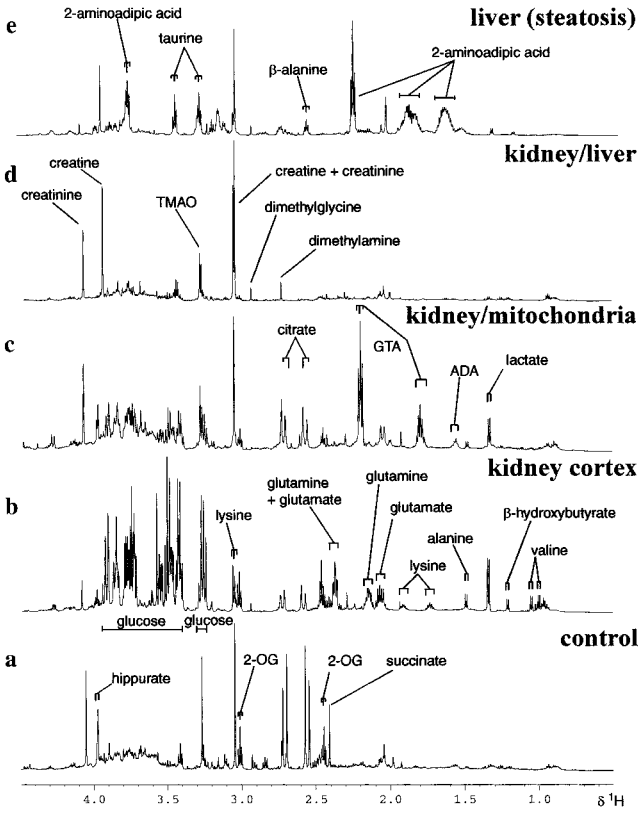

Figure 3. ^{1}H NMR spectra (600 MHz) of urine. Typical 600 MHz ^{1}H NMR spectra (δ 0.5−4.5) of urine obtained from a control rat (a) and rats treated with a single ip dose of selected tissue-specific toxins: hexachloro-1,2-butadiene (b), 2-bromoethanamine hydrochloride (c), thioacetamide (d), and hydrazine (e). Abbreviations: ADA, adipic acid; GTA, glutaric acid; 2-OG, 2-oxoglutarate; TMAO, trimethylamine *N*-oxide.

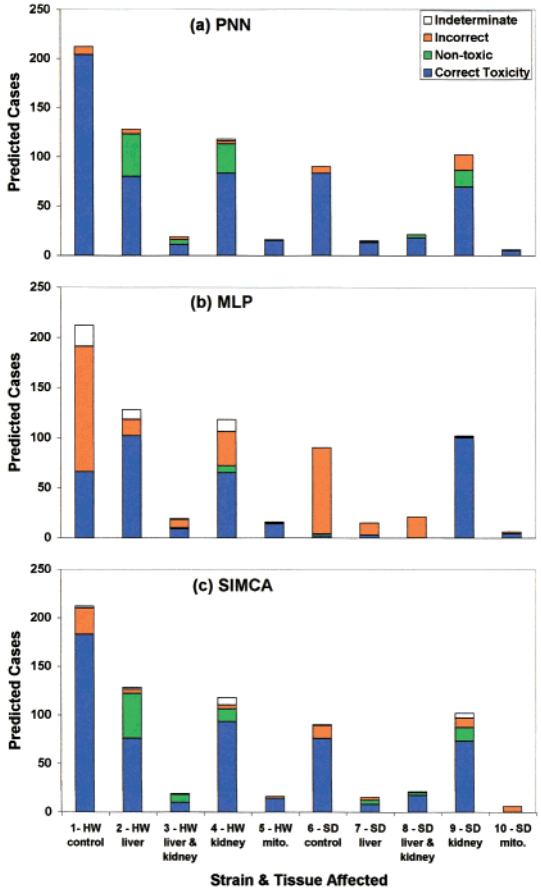

Figure 4. Results of initial PNN (a), MLP (b), and SIMCA (c) analysis. Bar chart showing the predicted class of organ and/or tissue toxicity and strain for a validation set of data (n = 727) from a PNN trained on a set of 583 samples. Key for toxicity type: 1-HW, control HW; 2-HW, HW liver toxin; 3-HW, HW liver and kidney toxin; 4-HW, HW kidney toxin; 5-HW, HW mitochondrial toxin; 6-SD, control SD; 7-SD, SD liver toxin; 8-SD, SD liver and kidney toxin; 9-SD, SD kidney toxin; 10-SD, SD mitochondrial toxin.

class, describing the probability of membership in each class. The probabilities will be greatest in regions where the spectra are characteristic of a given class, with diminishing values elsewhere (Figure 2a). Consequently, at any point in the space, i.e., any spectrum, the values of these probability distributions give the probability of membership of each of the classes for that spectrum. Thus, knowing these probability distributions allows the direct classification of any spectrum with the likelihood of it belonging to each class. These probability distributions can be approximated via PNNs using exemplar spectra and/or points of a training set (Figure 2b) around which Gaussian probability distributions are constructed (the "frog spawn" representation in Figure 2c). The theory of PNNs and their relationship to Bayesian probability distributions is well documented (*14*−*18*). We discuss here the potential of applying PNN analysis of NMR spectra to predicting the inherent toxicity of novel xenobiotics.

Materials and Methods

Animals and Treatments. Male Han Wistar or Sprague-Dawley rats (five to eight animals per group) were treated with either control vehicle (0.9% saline or corn oil) or one of the model toxins given in Table 1. All animals were acclimatized in grid-based plastic cages (five animals per cage) prior to group allocation. Each animal was placed in an individual metabolism cage in a well-ventilated room with a temperature of 21 ± 2 °C and a relative humidity of 50 ± 10% with a 12 h light/dark cycle. Food (Purina Rat Chow 5001) and water were provided ad libitum throughout the study. Urine samples were collected over ice at various time intervals over a 7 day period. Samples were centrifuged at 3000 rpm for 10 min to remove particulate contaminants, and the samples were stored at −40 °C pending NMR spectroscopic analysis. Samples collected between 0 and 8 h, 8 and 24 h, 24 and 32 h, 32 and 48 h, 48 and 72 h, and 72 and 96 h postdose (pd) were chosen for further analysis, except in the case of puromycin and adriamycin where samples from later time points (between 96 and 120 h and 120 and 144 h pd) were also used. Kidneys and liver samples were removed from all animals on termination, and histopathology was performed 48 and 168 h pd. The renal cortex was separated from the papilla by dissection. Tissue samples were fixed in 10% buffered formol saline, processed through paraffin wax, sectioned, stained with haematoxylin and eosin, and examined by light microscopy to confirm the nature and severity of the lesions by conventional histopathology.

Sample Preparation and ^{1}H NMR Spectroscopic Analysis of Urine. To minimize variations in the pH of the urine samples, 200 μL of 0.4 M phosphate buffer solution [Na_2HPO_4/NaH_2PO_4 (pH 7.4)] made up in ^2H_2O (to provide a field frequency lock) was mixed with 400 μL of urine in a microcontainer. The resulting solutions were left to stand for 10 min and then centrifuged at 13 000 rpm for 10 min to remove any precipitates. Each supernatant (500 μL) was placed into a 5 mm o.d. NMR tube (Wilmad 507PP). Conventional ^{1}H NMR spectra were measured at 600.13 MHz on a Bruker DRX-600 spectrometer at 303 K. The water resonance was suppressed using a presaturation pulse sequence (*28*) with irradiation during a 3 s relaxation delay and also during the 100 ms mixing time. Sixty-

Table 2. Initial Classification Studies (categories as in Table 1)

(a) Results of the Initial PNN Study (PNN1)

	Han Wistar					Sprague-Dawley				
	control (1)	liver (2)	kidney, liver (3)	kidney (4)	mito. (5)	control (6)	liver (7)	kidney, liver (8)	kidney (9)	mito. (10)
training set	179	100	17	103	16	69	10	14	72	3
validation set	212	128	19	118	16	90	15	21	102	6
validation set predictions										
correct toxicity	204	80	11	83	15	83	13	18	69	5
nontoxic		43	5	30			1	3	17	
incorrect	8	5	3	3	1	7	1		16	1
indeterminate				2						
% correct (including nontoxic)	96	96	84	96	94	92	93	100	84	83
total	94%									

(b) Results of the Initial MLP Study (MLP1)

	Han Wistar					Sprague-Dawley				
	control (1)	liver (2)	kidney, liver (3)	kidney (4)	mito. (5)	control (6)	liver (7)	kidney, liver (8)	kidney (9)	mito. (10)
training set	179	100	17	103	16	69	10	14	72	3
validation set	212	128	19	118	16	90	15	21	102	6
validation set predictions										
correct toxicity	66	102	9	65	14	2	3		100	4
nontoxic			1	7		2				
incorrect	125	16	8	34	1	86	12	21	1	2
indeterminate	21	10	1	12	1				1	
% correct (including nontoxic)	31	80	53	61	88	4	20	0	98	67
total	52%									

(c) Results of the Initial SIMCA Study (SIMCA1)

	Han Wistar					Sprague-Dawley				
	control (1)	liver (2)	kidney, liver (3)	kidney (4)	mito. (5)	control (6)	liver (7)	kidney, liver (8)	kidney (9)	mito. (10)
training set	179	100	17	103	16	69	10	14	72	3
validation set	212	128	19	118	16	90	15	21	102	6
validation set predictions										
correct toxicity	183	76	10	93	14	76	8	17	73	
nontoxic		46	8	13			4	3	14	
incorrect	27	4		4	2	13	3	1	10	6
indeterminate	2	2	1	8		1			5	
% correct (including nontoxic)	86	95	95	90	88	84	80	95	85	0
total	88%									

four free induction decays (FIDs) were collected into 64K data points using a spectral width of 7002.8 Hz, an acquisition time of 4.68 s, and a total pulse recycle delay of 7.68 s. Prior to Fourier transformation (FT), the FIDs were zero-filled to 128K and an exponential line broadening factor of 0.3 Hz was applied. All spectra were corrected for phase distortions and referenced to the methyl group of creatinine at δ 3.05. A baseline correction was also applied to each spectrum using a simple polynomial (up to fifth-order) curve fit.

NMR Data Reduction Procedures. Each NMR spectrum, between 0.2 and 10.0 ppm, was segmented into 246 regions 0.04 ppm in width using the software package AMIX (Analysis of MIXtures, version 2.0, Bruker Analytische Messtechnik, Rheinstetten, Germany). The optimal width of segmented regions was based on previous studies (*13*, *19*) which found that regions of 0.04 ppm accommodated any small pH-related shifts in signals and variation in shimming quality. To eliminate any spurious effects of variability in the suppression of the water resonance and any cross-relaxation effects on the urea signal via chemical exchange of the urea protons (*29*), the spectral region containing residual water and urea signals (δ 4.5−6.0) was removed. The model toxins selected for this study were well documented, and their metabolism was known. In general, compounds that either had no urinary metabolites or were excreted within the first 24 h following administration were chosen. Samples exhibiting significant presence of metabolites directly related to the administered compound were excluded from further analysis (i.e., adriamycin, puromycin aminonucleoside, dimethylhydrazine, thioacetamide, and ANIT at 0−8 h pd).

The integral was calculated for each of the resultant spectra, and these data were normalized to unit area. Each of these spectra can be considered as a multidimensional ($M = 207$) vector **p** which was subsequently employed in the neural network analyses and soft independent modeling of class analogy (SIMCA) analysis (Figure 1a). The data were classified initially on the basis of the target organ of toxicity. Subsequently, a more refined classification based on the exact site or type of toxicity was employed.

Neural Network Analyses. These data were then imported into the Statistica Neural Networks software ('99 Edition StatSoft) for analysis. The full data set was divided into two subsets: a training set ($n = 583$) and a validation set ($n = 727$). Care was taken to ensure that the validation set was independent of the training set, with spectra from any individual rat only appearing in one of the two sets. The training set was scaled such that the minimum and maximum values in each of the elements of the vectors were 0 and 1, respectively (the minimax option in Statistica NN) and this scaling factor employed thereafter for the validation set.

The multilayer perceptron network trained for the limited strain and tissue classification example employed a hidden layer consisting of 108 nodes (the mean of 207 input and 10 output nodes). This represents a typically sized network of this type; in principle, this network is able to distinguish a maximum of

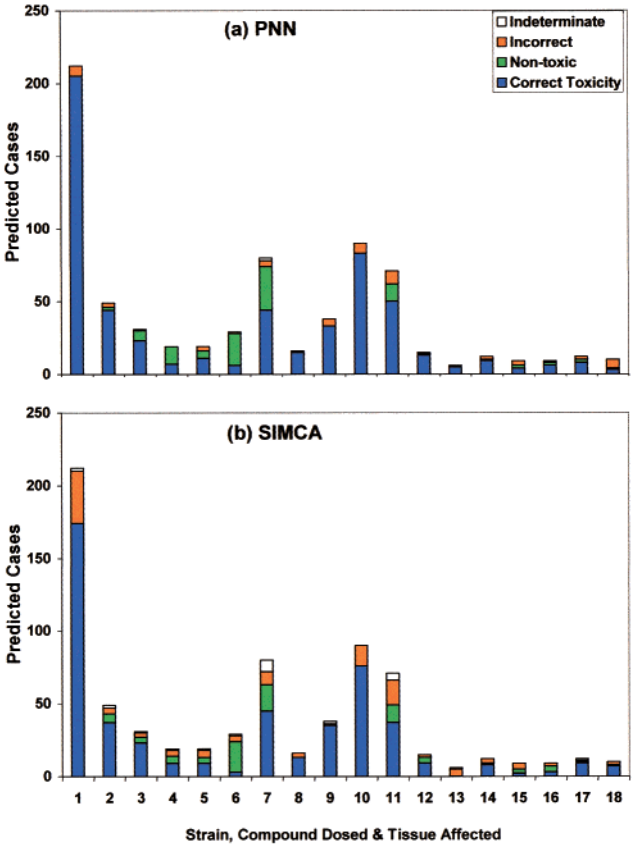

Figure 5. Results of refined PNN (a) and SIMCA (b) analysis. Bar chart of results from a refined PNN showing predicted class according to strain, administered compound, and tissue that has been affected. Key for toxicity type as in Table 1: 1, control HW; 2, HW hydrazine; 3, HW α-naphthyl isothiocyanate; 4, HW allyl alcohol; 5, HW thioacetamide; 6, HW dimethylhydrazine; 7, HW $HgCl_2$ and hexachlorobutadiene; 8, HW bromoethanamine at time periods relating to mitochondrial toxicity; 9, HW bromoethanamine at time periods relating to renal papillary toxicity; 10, control SD; 11, SD $HgCl_2$, uranyl nitrate, and hexachlorobutadiene; 12, SD lead acetate; 13, SD bromoethanamine at time periods relating to mitochondrial toxicity; 14, SD adriamycin; 15, SD puromycin at time periods relating to liver and renal tubular toxicity; 16, SD bromoethanamine at time periods relating to renal papillary toxicity; 17, SD puromycin at time periods relating to renal glomerular toxicity; 18, SD sodium fluoride

2^{108} linearly distinct classes. The network was trained using backward propagation, with care being taken to avoid overtraining.

The probabilistic neural networks for both the limited and refined examples utilized the same number of hidden nodes, consistent with the number of cases in the training set [this is dictated by the definition of PNNs (*15*−*17*)]. An optimal smoothing factor of 0.3 was employed, the only variable parameter within a PNN.

The final classifications, based on neural network outputs (both PNN and MLP), used an acceptance of 0.1 and rejection of 0.9 in the Statistica software (effective classification by highest probability).

To establish the improvement in classification achieved by probabilistic neural network analysis over more conventional chemometric analyses, SIMCA (a classification method based on principal components analysis) was performed on the normalized data in Pirouette (version 2.7, Infometrix, Seattle, WA).

PNN-Based Evaluation of the Time-Related Response to Toxicity. To exemplify the ability of the PNN analysis to define a time-related biochemical response associated with toxicities, a PNN was trained on a subsection of the data containing 28 samples pertaining to the low dose of HCBD at a predose time period and 8−24, 24−32, 32−48, 48−72, 72−96, and 96−120 h pd. A validation set of 26 samples was used to assess the ability of the PNN to classify the samples on the basis of collection time. These samples were obtained from eight animals (four for the training set and four for the validation set, with one from the training set and two from the validation set culled 48 h pd for the purposes of histopathology).

Results

^{1}H NMR urine spectra were generated for each animal over a 7 day time period (1310 spectra in total). Spectra from animals treated with a single dose of model toxin were compared to those obtained from the relevant control animals. Visual inspection of these spectra indicated that the biochemical composition of the urine varied in a manner related to the class of toxicity, dose, and time of sampling. Typical ^{1}H NMR urine spectra are shown in Figure 3. Previous ^{1}H NMR spectroscopic studies have identified specific spectral perturbations associated with particular classes of toxicity (*1*, *5*−*8*). However, the perturbations can be both complex and subtle, requiring pattern recognition techniques for extracting the full plethora of diagnostic information.

For this study, initially a PNN was trained using the training set of spectra ($n = 583$), classified according to histopathological evidence, to distinguish 10 classes of tissue toxicity and strain as defined in Table 1. Testing of this PNN with the validation set of spectra ($n = 727$) showed that it successfully predicted ∼94% of the cases with regard to strain and tissue toxicity (Figure 4a and Table 2a). Even when the control classes were discontinued, the success rate for sample prediction remained at a >92% level. In contrast to the high percentage of classification achieved by the PNN, analysis of the same data using a multilayer perceptron (MLP) network gave poor classification, achieving a success rate of 52% (Figure 4b and Table 2b). Furthermore, the MLP network was particularly poor at distinguishing between strains for control animals. Analysis of the data using soft independent modeling of class analogy (SIMCA), a classification technique based on principal components, gave classification that was much improved over the MLP network but was less successful than the PNN (Figure 4c and Table 2c). Correct classification for 88% of the validation cases was achieved. This advantage of PNNs stems primarily from their ability to differentiate cases which are ostensibly similar and which linear techniques such as PCA are unable to separate.

The greatest occurrence of apparent misclassification was found for SD rats treated with renal cortical toxins ($HgCl_2$, HCBD, and NaF). However, even for most of these cases, the site of toxicity was correctly classified as the kidney with the error residing in the prediction of strain. An idiosyncratic response was also found in ∼5% of the control samples. These correspond to metabolic outliers from animals that were not physiologically stable (e.g., stressed or sick animals). This appears to be a common occurrence in laboratory rats but is difficult to detect and monitor (*19*, *20*). Clearly, as these are not prescreened sets of rats, there will inevitably be a real distribution of anomalous behavior, which contributes to the overall 6% level of "misclassification". In practice, therefore, the *true* level of misclassification is somewhat lower than 6%.

Careful inspection of the PNN results reported here identified those cases either where the rat had recovered

Table 3. Refined Classification Studies (categories as in Table 1)

(a) Results of the Refined PNN Study (PNN2)

	Han Wistar										Sprague-Dawley							
	control (1)	hydrazine (2)	ANIT (3)	allyl alcohol (4)	thioacetamide (5)	DMH (6)	$HgCl_2$/HCBD (7)	BEA (mito.) (8)	BEA (RPN) (9)	control (10)	$HgCl_2$/HCBD/UN (11)	PbAc (12)	BEA (mito.) (13)	adriamycin (14)	PAN (kidney, liver) (15)	BEA (RPN) (16)	PAN (glom.) (17)	NaF (18)
training set	179	30	26	17	17	27	73	16	30	69	49	10	3	8	6	7	7	9
validation set	212	49	31	19	19	29	80	16	38	90	71	15	6	12	9	9	12	10
validation set predictions																		
correct toxicity	205	44	23	7	11	6	44	15	33	83	50	13	5	9	4	6	8	3
nontoxic		2	7	12	5	22	30				12	1		1	2	2	2	1
incorrect	7	3	1		3	1	4	1	5	7	9	1	1	2	3	1	2	6
indeterminate							2											
% correct (including nontoxic)	97	94	97	100	84	97	93	94	87	92	87	93	83	83	67	89	83	40
total	92%																	

(b) Results of the Refined SIMCA Study (SIMCA2)

	Han Wistar										Sprague-Dawley							
	control (1)	hydrazine (2)	ANIT (3)	allyl alcohol (4)	thioacetamide (5)	DMH (6)	$HgCl_2$/HCBD (7)	BEA (mito.) (8)	BEA (RPN) (9)	control (10)	$HgCl_2$/CBD/UN (11)	PbAc (12)	BEA (mito.) (13)	adriamycin (14)	PAN (kidney, liver) (15)	BEA (RPN) (16)	PAN (glom.) (17)	NaF (18)
training set	179	30	26	17	17	27	73	16	30	69	49	10	3	8	6	7	7	9
validation set	212	49	31	19	19	29	80	16	38	90	71	15	6	12	9	9	12	10
validation set predictions																		
correct toxicity	174	37	23	9	9	3	45	13	35	76	37	9		8	2	3	9	7
nontoxic		6	4	5	4	21	18				12	4		1	3	4	1	1
incorrect	36	4	3	4	5	4	9	3	1	14	17	2	5	3	4	2	1	2
indeterminate	2	2	1	1	1	1	8		2		5		1				1	
% correct (including nontoxic)	82	88	87	74	68	83	79	81	92	84	69	87	0	75	56	78	83	80
total	80%																	

Table 4. Results of the PNN Study of the HCBD Toxicity Time Course

	predose	8−24 h pd	24−32 h pd	32−48 h pd	48−72 h pd	72−96 h pd	96−120 h pd
training set	7	4	4	4	3	3	3
validation set	8	4	4[a]	4	2	2	2
predicted time of sampling							
predose	8	0	0	0	0	0	0
8−24 h pd	0	3	1	0	0	0	0
24−32 h pd	0	0	2	2	0	0	0
32−48 h pd	0	1	0	2	0	0	0
48−72 h pd	0	0	0	0	2	0	0
72−96 h pd	0	0	0	0	0	1	0
96−120 h pd	0	0	0	0	0	1	2

[a] One indeterminate outlier.

from a single administration of compound or where the onset of toxicity had not commenced. For example, Han Wistar rats treated with DMH and allyl alcohol exhibited only modest hepatic lesions and recovered rapidly to produce "control-like" profiles midway through the study.

As follows from the success of the PNN described above, another network was trained using the training set of spectra ($n = 583$), classified according to a more refined histopathological grading, to distinguish 18 classes of tissue toxicity, mechanism, and strain (Table 1). Here, the successful classification of the validation set remained at a level of >92% of the cases (Figure 5a and Table 3a). The success rate for prediction of classes remained at >89% even if the control classes were discounted. Again, this compared favorably with the result of approximately 50% of successful classification using a MLP network (data not shown) and 80% using SIMCA analysis (Figure 5b and Table 3b). Thus, we have shown that PNN analysis can give substantial improvement in classification power.

As with the simpler classification scheme, rapid recovery or slow onset of toxicity was correctly identified in the PNN analysis. The only significant anomaly was found with the classification of NaF as $HgCl_2$/HCBD/UN toxicity and vice versa. Whereas Hg, HCBD, and UN specifically target the S3 portion of the proximal tubule, NaF induces a more widespread proximal tubular lesion (which incorporates the S3 portion). It can be supposed either that initial damage to the S3 region via $HgCl_2$, HCBD, and UN has become more widespread over the time period or that the distinction between the adjacent regions of the proximal tubule is not sufficiently well characterized in the urine spectra.

A PNN was used to predict the metabolic response of a subsection of animals in relation to time. On the basis of samples obtained from HW rats treated with a small dose of the renal cortical toxin HCBD, a clear time-dependent biochemical response could be defined. Moreover, the time of sampling following the administration of HCBD was predicted successfully for all validation samples ($n = 26$), to within 24 h of the correct time of collection (Table 4).

Discussion

Previous use of chemometric analysis of ^{1}H NMR spectroscopic data in metabonomic toxicological studies has been successful in distinguishing major classes of tissue toxicity, in some cases with resolved mechanistic detail (*11, 12, 21, 22*). Early studies employing chemometric analysis of NMR data relied on scoring or quantifying selected metabolites, thereby making an assumption about the relative importance of certain metabolites as descriptors of toxicity; basic classification of liver, renal cortical, renal medullary, and testicular toxicity was achieved, using PCA (*9*), nonlinear mapping (*11*), and multilayer perceptron NNs (*12*). The more refined approach adopted in subsequent studies, whereby the whole spectrum was digitized and used for classification, allowed further definition of classes of toxicity (*21*−*24*). However, to date, the chemometric methods that have been applied (e.g., PCA, SIMCA, mulilayer perceptron NNs, and cluster analysis) have only been able to reliably classify broad categories of tissue-specific toxicity on subsets of these data.

Here we were able to achieve effective classification over a wider and more refined variety of classes while still retaining more than 55% of these data for independent validation. It should be emphasized that the classification derives from the inherent modification and differences in metabolic profile, not the mere presence of compound metabolites, as samples containing NMR detectable levels of such were specifically eliminated from analysis.

From the study presented here, it is evident that the two strains of standard laboratory rat (SD and HW) can be distinguished from each other simply on the basis of NMR metabonomic profile by PNN, irrespective of whether a toxic insult has been administered. This is particularly significant given that HW and SD rat strains are closely related genetically. Previous work has shown that control SD and HW rats can be differentiated by SIMCA analysis of their ^{1}H NMR urine spectra (*13*). However, we have shown here that strain-related differences in metabolic response to xenobiotics can also be characterized using the more sensitive technique of PNN analysis. This would suggest that metabonomic NMR analysis will provide a powerful tool for identifying metabolic changes due to genetic variation and may be of use in validating animal models for human disease and toxicological phenomena. Furthermore, the method can identify metabolic outliers and physiologically anomolous animals, allowing improved interpretation of toxicological data and prescreening in animal studies.

Toxic lesions are dynamic processes that evolve over time and have proven to be difficult for other chemometric methods to deconvolve, although time trajectories of toxicological responses for selected toxins have been reported (*20, 21*). The sensitivity of PNNs indicates that they are likewise able to elucidate the time course of toxicological response. The ability of PNNs to define a time-related biochemical profile following a toxic insult was exemplified using the subset of the data relating to samples obtained from HW rats treated with a small dose of the renal cortical toxin HCBD. Thus, this methodology

may be of value in establishing the time or stage of toxicity or disease processes.

In addition to classification, the biochemical factors contributing to the classification can be established. For example, 2-bromoethanamine hydrobromide (BEA) causes two distinct types of toxicity. Glutaric acid was found to heavily influence the classification of samples from BEA-treated animals up to 48 h pd. Glutaric acid excretion is known to be associated with a mitochondrial lesion arising from inhibition of fatty acyl CoA dehydrogenase enzymes (*25*). At later time periods, classification of samples from BEA-treated animals was influenced by urinary levels of trimethylamine *N*-oxide, dimethylglycine, and creatine, which together indicate a perturbation in renal medullary function (*21*). The identification of biomarkers of organ-specific toxicity can allow insight into the mechanisms of toxicity (*5*−*7*).

The search for clinical biomarkers indicating target organ toxicity in humans is hindered by variation in factors such as genetic composition, diet, age, and idiosyncratic responses to drugs. Moreover, model compounds seldom target a single organ or tissue in isolation, and therefore, biofluid composition will reflect the overall response of an organism. In the study presented here, we have shown that using PNNs, not only is it possible to predict the target organ toxicity of certain compounds on the basis of their NMR-based urine profiles but it is also possible to classify the effects of multiple target organ toxicities. For example, samples obtained from the model toxin 2-bromoethanamine were classified under mitochondrial toxicity (for samples obtained between 0 and 24 h pd) and renal papillary toxicity (in the case of samples obtained beyond 24 h pd).

We have established that ^{1}H NMR urine spectra contain sufficient information to distinguish not only the organ that has been affected but also sites within the organ following toxic insult. Furthermore, we have shown that the PNN classification method is significantly more successful than the previously employed methods in extracting this information. Of particular relevance is the ability of PNN-based metabonomic profiling of urine to distinguish differences between different "wild type" rat strains with respect to normal physiological metabolism and their response to toxic insult. NMR-based metabonomics may be of great biological significance in studying genetic differences, including those due to specific intervention or engineering. This is supported by the earlier use of ^{1}H NMR as a means of investigating inborn errors of metabolism in humans (*26*, *27*) which are the result of specific genetic defects. Moreover, the technique may be of use in validating animal models of human disease processes and toxicological phenomena using metabonomic criteria. Once established, such criteria could be further adapted to the investigation of the efficacy of novel drugs based on the success of normalization of the perturbed metaboilc profile. Finally, it is clear that there is a high degree of complementarity between proteomic, transcriptomic, and metabonomic methods, and that the integrated use of these approaches will provide a holistic picture of an organism's overall response to toxic or physiological challenges.

Acknowledgment. We are grateful to SmithKline Beecham and GlaxoWellcome for funding and providing facilities. We also thank Dr. Andrew Nicholls for providing data on Han Wistar rats.

References

(1) Nicholson, J. K., Lindon, J. C., and Holmes, E. (1999) 'Metabonomics': understanding the metabolic responses of living systems to pathophysiological stimuli via multivariate statistical analysis of biological NMR spectroscopic data. *Xenobiotica* **11**, 1181−1189.

(2) Sinclair, B. (1999) Everything's Great When It Sits on a Chip: A bright future for DNA arrays. *Scientist* **13**, 11 18−20.

(3) Geisow, M. J. (1998) Proteomics: One small step for a digital computer, one giant leap for humankind. *Nat. Biotechnol.* **16**, 206.

(4) Anderson, N. L., Taylor, J., Hofmann, J. P., Esquer-Blasco, R., Swift, S., and Anderson, N. G. (1996) Simultaneous measurement of hundreds of liver proteins: application in assessment of liver function. *Toxicol. Pathol.* **24**, 72−76.

(5) Gartland, K. P. R., Bonner, F. W., and Nicholson, J. K. (1989) Investigations into the biochemical effects of region-specific nephrotoxins. *Mol. Pharmacol.* **35**, 242−250.

(6) Nicholson, J. K., Timbrell, J. A., and Sadler, P. J. (1985) Proton NMR spectra of urine as indicators of renal damage: Mercury nephrotoxicity in rats. *Mol. Pharmacol.* **27**, 644−651.

(7) Sanins, S. M., Timbrell, J. A., Elcombe, C. R., and Nicholson, J. K. (1990) Hepatotoxin-induced hypertaurinuria: a proton NMR study. *Arch. Toxicol.* **64**, 407−411.

(8) Nicholson, J. K., and Wilson, I. D. (1989) High-resolution proton NMR spectroscopy of biological fluids. *Prog. NMR Spectrosc.* **21**, 444−501.

(9) Gartland, K. P. R., Beddell, C., Lindon, J. C., and Nicholson, J. K. (1991) The application of pattern recognition methods to the analysis and classification of toxicological data derived from NMR spectroscopy of urine. *Mol. Pharmacol.* **39**, 629−642.

(10) Howells, S. L., Maxwell, R. J., Peet, A. C., and Griffiths, J. R. (1992) An investigation of tumour ^{1}H nuclear magnetic resonance spectra by the application of chemometric techniques. *Magn. Reson. Med.* **28**, 214−236.

(11) Gartland, K. P. R., Sanins, S. M., Nicholson, J. K., Sweatman, B. C., Beddell, C. R., and Lindon, J. C. (1990) Pattern recognition analysis of high resolution ^{1}H NMR spectra of urine. A nonlinear mapping approach to the classification of toxicological data. *NMR Biomed.* **3**, 166−172.

(12) Anthony, M. L., Rose, V. S., Nicholson, J. K., and Lindon, J. C. (1995) Classification of toxin-induced changes in ^{1}H NMR spectra of urine using an artificial neural network. *J. Pharm. Biomed. Anal.* **13**, 205−211.

(13) Holmes, E., Nicholls, A. W., Lindon, J. C., Ramos, S., Spraul, M., Neidig, P., Connor, S. C., Connelly, J., and Nicholson, J. K. (1998) Development of a model for classification of toxin-induced lesions using ^{1}H NMR spectroscopy of urine combined with pattern recognition. *NMR Biomed.* **11**, 235−244.

(14) Parzen, E. (1962) On estimation of a probability density function and mode. *Ann. Math. Stat.* **33**, 1065−1076.

(15) Bishop, C. (1995) *Neural Networks for Pattern Recognition*, pp 164−193, University Press, Oxford, U.K.

(16) Speckt, D. F. (1990) Probabilistic neural networks. *Neural Networks* **3** (1), 109−118.

(17) Broomhead, D. S., and Lowe, D. (1988) Multivariate functional interpolation and adaptive networks. *Complex Syst.* **2**, 321−355.

(18) Patterson, D. (1996) *Artificial Neural Networks*, Prentice Hall, Singapore.

(19) Holmes, E., Nicholls, A. W., Lindon, J. C., Connor, S. C., Connelly, J. C., Haselden, J. N., Damment, S. J. P., Spraul, M., Neidig, P., and Nicholson, J. K. (2000) Chemometric Models for Toxicity Classification Based on NMR Spectra of Biofluids. *Chem. Res. Toxicol.* **13** (6), 771−778.

(20) Phipps, A. N., Stewart, J., Wright, B., and Wilson, I. D. (1998) Effect of diet on the urinary excretion of hippuric acid and other dietary-derived aromatics in rat. A complex interaction between diet, gut microflora and substrate specificity. *Xenobiotica* **28**, 527−537.

(21) Holmes, E., Bonner, F. W., Sweatman, B. C., Lindon, J. C., Beddell, C. R., Rahr, E., and Nicholson, J. K. (1992) Nuclear magnetic resonance spectroscopy and pattern recognition analysis of the biochemical processes associated with the progression and recovery from nephrotoxic lesions in the rat induced by mercury II chloride and 2-bromoethanamine. *Mol. Pharmacol.* **42**, 922−930.

(22) Beckwith-Hall, B. M., Nicholson, J. K., Nicholls, A. W., Foxall, P. J. D., Lindon, J. C., Connor, S. C., Abdi, M., Connelly, J., and Holmes, E. (1998) Nuclear magnetic resonance spectroscopic and

principal components analysis investigations into biochemical effects of three model hepatotoxins. *Chem. Res. Toxicol.* **11**, 260−272.
(23) Farrant, R. D., Lindon, J. C., Rahr, E., and Sweatman, B. C. (1992) An automatic data reduction and transfer method to aid pattern recognition analysis and classification of NMR spectra. *J. Pharm. Biomed. Anal.* **10**, 141−144.
(24) El-Deredy, W. (1997) Pattern recognition approaches in biomedical and clinical magnetic resonance spectroscopy: a review. *NMR Biomed.* **10**, 99−124.
(25) Golden, K. D., and Kean, E. A. (1984) The biogenesis of dicarboxylic acid in rats given hypoglycin. *Biochim. Biophys. Acta* **794** (1), 83−88.
(26) Iles, R. A., and Chalmers, R. A. (1988) Nuclear magnetic resonance spectroscopy in the study of inborn errors of metabolism. *Clin. Sci.* **74**, 1−10.
(27) Holmes, E., Foxall, P. J. D., Spraul, M., Farrant, R. D., Nicholson, J. K., and Lindon, J. C. (1997) 750 MHz ^{1}H NMR spectroscopic characterisation of the complex metabolic pattern of urine from patients with inborn errors of metabolism: 2-hydroxyglutaric aciduria and maple syrup urine disease. *J. Pharm. Biomed. Anal.* **15**, 1647−1659.
(28) Nicholson, J. K., Foxall, P. J. D., Spraul, M., Farrant, R. D., and Lindon, J. C. (1995) 750 MHz ^{1}H and ^{1}H-^{13}C NMR spectroscopy of human blood plasma. *Anal. Chem.* **67** (5), 793−811.
(29) Connor, S. C., Nicholson, J. K., and Everett, J. R. (1987) Chemical-exchange and paramagnetic T2 relaxation agents for water suppression in spin−echo proton nuclear magnetic resonance spectroscopy for biological fluids. *Anal. Chem.* **59**, 2885−2891.

TX000158X